Check for updates

Metal-free photoredox-catalyzed direct α-oxygenation of *N,N*-dibenzylanilines to imides under visible light†

Nalladhambi Neerathilingam and Ramasamy Anandhan [iD] *

An efficient synthesis of imides using metal-free photoredox-catalyzed direct α-oxygenation of *N,N'*-disubstituted anilines in the presence of 9-mesityl-10-methylacridinium [Acr$^+$-Mes]BF$_4$ as a photoredox catalyst and molecular oxygen as a green oxidant under visible light was developed. This photochemical approach offered operational simplicity, high atom economy with a low E-factor, and functional group tolerance under mild reaction conditions. Control and quenching experiments confirmed the occurrence of a radical pathway and superoxide radical anion α-oxygenation reactions, and also provided strong evidence for the reductive quenching of [Acr$^+$-Mes]BF$_4$ based on a Stern–Volmer plot, which led to the proposed mechanism of this reaction.
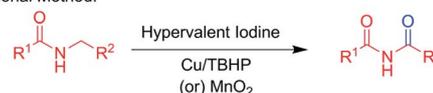
Introduction

Imides are versatile building blocks in many organic syntheses[6] and also have many potential important applications in pharmaceuticals,[1,2] agrochemicals,[3] material science,[4] and organic photovoltaics.[5] Because of the importance of imides, various strategies have been established[6–9] for synthesizing them, including the Mumm rearrangement of isoimides,[10–12] oxidative acylation reactions,[13] transition metal carbonylative coupling reactions, C–H/N–H coupling reactions, three-component coupling reactions,[14–17] *etc.* Of these strategies, the direct α-oxygenation of amines has brought special attention to the scientific community due to the easy availability of amines and the environmental friendliness of the approach.[18] Direct α-oxygenation of *N*-alkyl amides to imides using hypervalent iodine, Cu/TBHP and MnO$_2$ (Scheme 1a) has previously been reported[13,19–21] – but has been found to require the use of transition metals and a stoichiometric amount of oxidants, and to produce a very large amount of by-products with a high E-factor. Therefore, the use of clean oxidants is essential to minimize the quantity and toxicity of the released waste. In this regard, thus the use of molecular oxygen as a simple, green and environment friendly oxidant has fulfilled the requirements with high atom economy, low E-factor and producing water as a by-product.[22]

In recent years, visible-light-mediated metal-free photo-catalyzed oxygenation reactions using molecular oxygen as a green oxidant have become increasingly important in many organic syntheses,[23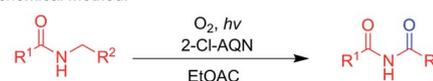] due to the ability of these reactions to activate O$_2$ into highly reactive oxygen species such as singlet oxygen (^{1}O$_2$) and superoxide radical anion (O$_2$$^{\cdot-}$) using energy transfer (ET) or photoinduced electron transfer (PET) processes. One such work published in 2018 by S. Das *et al.* demonstrated visible-light-mediated metal-free photoredox-catalyzed α-oxygenation of *N*-benzyl amine by O$_2$ as an oxidant, and this strategy has also been applied to the synthesis of phthalimides from isoindoline.[24] In 2014, Akichika and co-workers reported 2-chloroanthraquinone-catalyzed aerobic photo-oxidations of diacylamines (Scheme 1b).[25] Recently, our group established visible-light-induced metal-involved and metal-free photo-catalyzed organic transformations deploying molecular oxygen as a green oxidant.[26] Also, our group has published work on the α-oxidation of *N,N*-dibenzylanilines to amides *via* oxidative C–N cleavage as a prominent product in the presence of rose bengal

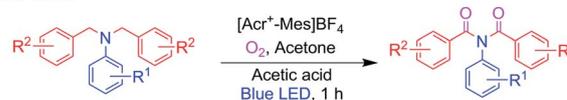*Department of Organic Chemistry, University of Madras, Chennai 600025, India.*
E-mail: ananthanramasamy@gmail.com

† Electronic supplementary information (ESI) available: Spectral data for all new compounds. See DOI: 10.1039/d2ra00585a

Scheme 1 Various strategies involving α-oxygenation reactions of amides and amines for synthesizing imides.

as a photocatalyst and O_2.[26d] However, to the best of our knowledge, direct α-oxygenation of amines to imides has not yet been reported. Hence, we set out to work on and achieved a visible-light-induced α-oxygenation of *N,N*-dibenzylanilines to imides as prominent products in the presence of [Acr+-Mes]BF$_4$ as a photocatalyst and O_2 (Scheme 1).

Experimental section

General considerations

The acquired ^{1}H and ^{13}C NMR spectra were recorded in CDCl$_3$ using a Bruker 300 MHz NMR spectrometer with TMS as an internal standard (see ESI†). Mass spectra were recorded using a Xevo G2S Q-TOF spectrometer (see ESI†). The light source for photochemical reactions was a Kessil 456 nm-wavelength blue light-emitting diode (LED) (see ESI Fig. S1†) (model number: KSPR160L-456-EU). LEDs producing light of different wavelengths including 370 nm, 390 nm, 467 nm and 527 nm were purchased from Kessil and were also used. Reaction tubes made of borosilicate glass were used as reaction vessels. The distance between the light source and the reaction vessel was 8 cm. TLC was performed using Merck pre-coated TLC plates (Merck 60 F254) and the results were visualized using UV light. Column chromatographic separation was carried out with silica gel (100–200 mesh). Reagents and solvents were purified as per standard procedures and used.

General experimental procedure

General procedure A for the synthesis of *N,N*-dibenzylanilines.[29] To a mixture of anilines (10 mmol) and K$_2$CO$_3$ (20 mmol) in DMF, benzylbromide (30 mmol) was added dropwise. The reaction was stirred at room temperature overnight. Water was added to the mixture and extracted with ethyl acetate twice. The resulting combined organic phase was washed with brine and dried over Na$_2$SO$_4$. The resulting concentrated residue was purified by performing column chromatography over silica gel using EtOAc/hexanes (1 : 9) as eluent to furnish the corresponding *N,N*-dibenzylanilines.

Procedure B for the preparation of imides. The reaction tube was charged with *N,N*-dibenzylanilines (0.36 mmol), acetic acid (1.8 mmol), and [Acr+-Mes]BF$_4$ (5 mol%) in acetone (8 mL). The resulting reaction mixture was stirred in the presence of O_2 (balloon) under blue light for 1 h. After the reaction was completed, the solvent was evaporated under reduced pressure. The resulting crude product was purified by performing column chromatography using EtOAc/hexanes as eluent to furnish the corresponding imide compounds (see ESI† for NMR data of the products).

Results and discussion

To examine the feasibility of the proposed method, *N,N*-dibenzylaniline **1a** was selected as a model substrate for optimizing the reaction conditions as shown in Table 1. The model substrate **1a** was irradiated with blue LED$_{456nm}$ light under O_2 in acetone for 35 h to afford the *N*-benzoyl-*N*-phenylbenzamide **2a** and phenylbenzamide **2a'** in 20% and 32% yields, respectively. The yield

of product **2a** was reduced when the reactions were carried out in, respectively, DMSO, toluene, and ACN instead of acetone (Table 1, entries 2–4). There was no significant improvement in the yields on the screening of other light sources. Namely LEDs producing light of wavelengths of, respectively, 370 nm, 390 nm, 467 nm, and 525 nm (Table 1, entries 5–8). The use of photoredox catalysts such as methylene blue, eosin Y and [Acr+-Mes]BF$_4$ was screened for further optimization (Table 1, entries 9–11). Gratifyingly, the regioselective product **2a** was obtained as a predominant product with a 41% yield in [Acr+-Mes]BF$_4$ as a photocatalyst (Table 1, entry 11). Interestingly, the best yield of **2a**, which was 71%, was obtained when carrying out the reaction for 1 hour with the addition of 1.8 mmol of acetic acid as an additive (Table 1, entry 12). Further screening of other acids such as H$_2$SO$_4$ and PTSA led in each case to a lower yield of product **2a** (Table 1, entries 13 and 14). Control experiments indicated that [Acr+-Mes]BF$_4$, acetic acid, and molecular oxygen were all needed to furnish imides (Table 1, entries 15–17).

Having optimized the reaction conditions, we investigated the *N,N*-dibenzylaniline substrate scope, and Scheme 2 summarizes the findings. The R^1 substituents including H, 4-CH$_3$ and 4-CH(CH$_3$)$_2$ on anilines **1a–c** reacted smoothly to give the corresponding imides **2a–c** in good yields. Reaction of the 4-F, 4-Cl, 3-Cl, 2-Br, and 4-Br halogen substituents on the anilines, namely **1d–h**, under optimized conditions afforded the imides **2d–h** in 70–92% yields. Furthermore, the 4-CN, 4-COCH$_3$, 3-NO$_2$, and 4-NO$_2$ electron-withdrawing groups on anilines **1i–l** afforded the corresponding products **2i–l**, but did so in lower yields. And heteroaryl amine **1m** and aliphatic amine **1n** failed to produce the respective products **2m** and **2n** under the optimized conditions.

Furthermore, to extend the substrate scope, the R^2 substituent on the benzyl aromatic ring of the *N,N*-dibenzylaniline was investigated as shown in Scheme 3. Various such substituents (2-Me, 4-Me, 4-F, 3-Cl and 4-Cl) on *N,N*-dibenzylamines **3a–e** were reacted under optimized conditions to afford the corresponding imides **4a–e** in 53–70% yields, respectively. Interestingly, the unsymmetrical *N,N*-dibenzylaniline **3f** also afforded the corresponding product, namely **4f**, in good yield. In contrast, the electron-withdrawing substituents 4-NO$_2$ and 2-CN on *N,N*-dibenzylamines **3g** and **3h** failed to produce imides **4g** and **4h**.
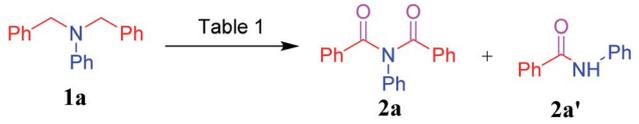
$$\text{Atom economy}(\%) = \frac{\text{Molecular mass of desired product}}{\text{Molecular mass of all reactants}} \times 100$$

$$\text{Reaction mass efficiency }(\%) = \frac{\text{Mass of desired product}}{\text{Mass of all reactants}} \times 100$$

$$\text{Product yield} = 68\%$$

$$\text{E-factor} = \frac{1.3 \text{ g} + 1.5 \text{ g} + 25.52 \text{ g} - (0.97 \text{ g} + 15.75 \text{ g})}{0.6 \text{ g}}$$

Table 1 Optimization of the α-oxygenation of N,N-dibenzylaniline (**1a**) to N-benzoyl-N-phenylbenzamide (**2a**)[a]

Entry	Light source (nm)	PC	Additive	Solvent	Yields[b] (%) 2a	2a'
1	456 (44 W)	—	—	Acetone	20	32
2	456 (44 W)	—	—	ACN	10	25
3	456 (44 W)	—	—	Toluene	0	0
4	456 (44 W)	—	—	DMSO	0	0
5	370 (43 W)	—	—	Acetone	15	15
6	390 (52 W)	—	—	Acetone	15	22
7	467 (44 W)	—	—	Acetone	Trace	15
8	525 (44 W)	—	—	Acetone	0	10
9	456 (44 W)	MB	—	Acetone	Trace	35
10	456 (44 W)	Eosin Y	—	Acetone	9	23
11	456 (44 W)	[Acr+-Mes]BF4	—	Acetone	41	8
12	456 (44 W)	[Acr+-Mes]BF4	AcOH	Acetone	75	0
13	456 (44 W)	[Acr+-Mes]BF4	H2SO4	Acetone	0	0
14	456 (44 W)	[Acr+-Mes]BF4	PTSA	Acetone	0	0
15[c]	456 (44 W)	[Acr+-Mes]BF4	AcOH	Acetone	50	0
16[d]	456 (44 W)	[Acr+-Mes]BF4	AcOH	Acetone	n.r.	n.r.
17[e]	—	[Acr+-Mes]BF4	AcOH	Acetone	n.r.	n.r.

[a] Reaction conditions: for each experiment, a mixture of **1a** (0.36 mmol), additive (1.8 mmol), and PC (5 mol%) in 8 mL of solvent was irradiated with blue LED light under an O_2 atmosphere at rt. [b] Isolated yields. [c] Reaction was performed under air. [d] Reaction was performed under N_2. [e] Reaction was performed in the dark. Abbreviations: n.r. = no reaction, PC = photocatalyst, MB = methylene blue, [Acr+-Mes]BF4 = 9-mesityl-10-methylacridinium tetrafluoroborate, AcOH = acetic acid, and PTSA = p-toluenesulfonic acid.

E-factor = 11.6 kg waste/1 kg product

$$\text{Atom economy} = \frac{301}{305} \times 100 = 98.6\%$$

$$\text{Atom efficiency} = \frac{98.6\% \times 68\%}{100} = 67\%$$

$$\text{Carbon efficiency} = \frac{20}{20} \times 100 = 100\%$$

$$\text{Reaction mass efficiency} = \frac{0.97\ \text{g}}{1.3\ \text{g}} \times 100 = 74.6\%$$

To determine the efficiency of this visible-light-mediated α-oxygenation reaction, a scaled-up reaction was performed with **1a** (1.3 g, 5 mmol) and AcOH (1.5 g, 25 mmol) under optimized conditions, and afforded the corresponding N-benzoyl-N-phenylbenzamide **2a** (0.97 g, 68%) (Scheme 4). Furthermore, we evaluated green chemistry metrics[27] for the synthesis of imide **2a**. This evaluation showed an E-factor of 11.6, a high atom economy of 98.6%, atom efficiency of 67%, carbon efficiency of 100%, and reaction mass efficiency of 74.6% (Table 2).

To acquire mechanistic insights, several control and quenching experiments were performed as shown in Scheme 5. The reaction performed with N-benzyl-N-phenylbenzamide 5 under optimized conditions afforded a 0% yield of **2a** (Scheme 5a), implying that the reaction did not involve formation of reactive intermediates of N-benzyl-N-phenylbenzamide 5. The quenching experiments, shown in Scheme 5b, were specifically carried out to understand the involvement of reactive oxygen species and the mechanism of the α-oxygenation reaction.[28] Under optimized conditions, reactions of 2,2,6,6-tetramethyl-1-piperidinyloxyl (TEMPO), benzoquinone (BQ) and sodium azide (NaN₃) afforded, respectively, 0%, trace, and 75% yields of **2a**. These results clearly indicated the involvement of a radical as well as superoxide radical anion in the photocatalytic α-oxygenation reaction and it also indicated no involvement of singlet oxygen in the reaction pathway. Further confirmation of the involvement of superoxide radical anion using EPR spectroscopy is shown in Fig. 1. An ESR spectrum was recorded after a solution of 5,5-dimethyl-pyrroline-N-oxide (DMPO) (0.02 mL), N,N-dibenzylaniline **1a** (0.36 mmol), AcOH (1.8 mmol), and Acr+-Mes (5 mol%) in acetone (8 mL) under an O_2 atmosphere was irradiated with blue LED$_{456nm}$ light for 5 minutes. Six strong signals characteristic of DMPO–OOH were observed. In the absence of light, no signal was observed when the reaction with DMPO was conducted (Fig. 1).
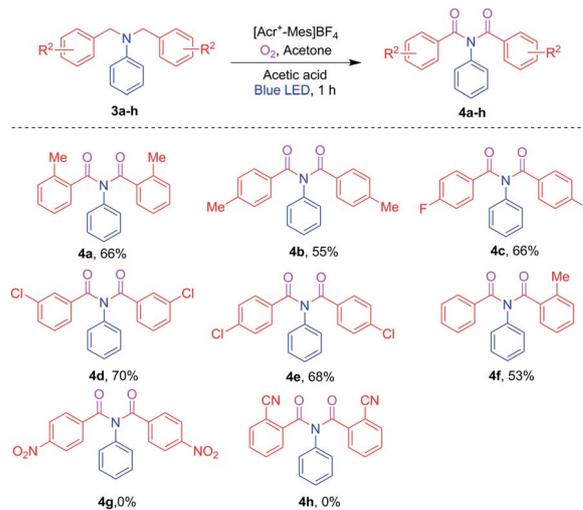
Paper
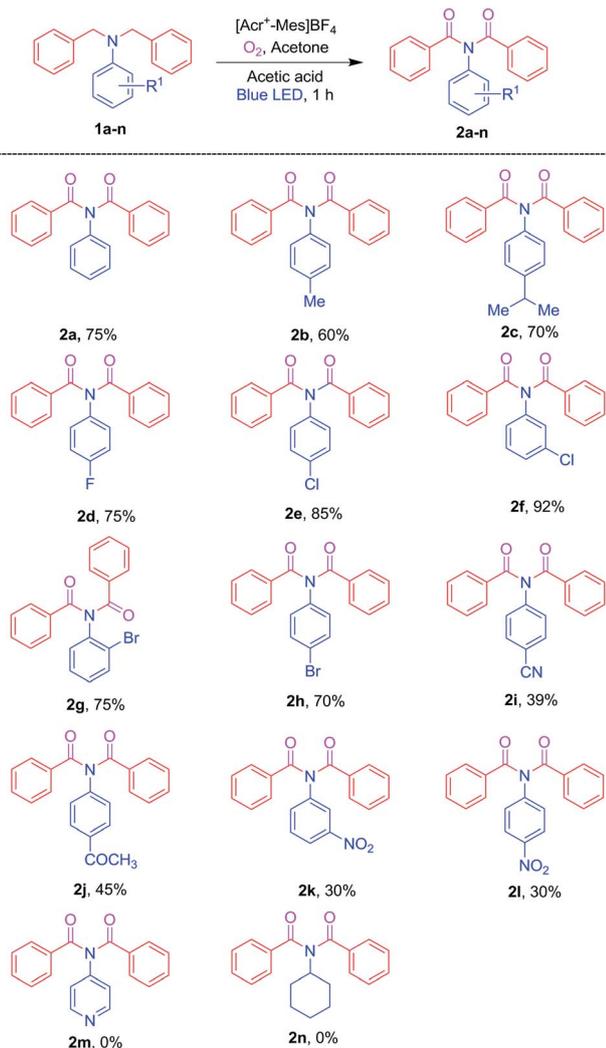
Scheme 2 Testing of various R^1 substituents on *N,N*-dibenzylanilines for the imide-producing reaction. [a] Reaction conditions: for each experiment, a mixture of an aniline (1a–n, 0.36 mmol), AcOH (1.8 mmol), and [Acr$^+$-Mes]BF$_4$ (5 mol%) in 8 mL acetone was irradiated with blue LED$_{456nm}$ light under O$_2$ at rt for 1 h. Yields were determined after purification.

Scheme 3 Testing of various R^2 substituents on *N,N*-dibenzylanilines for the imide-producing reaction. [a] Reaction conditions: for each experiment, a mixture of an aniline (3a–h, 0.36 mmol), AcOH (1.8 mmol), and [Acr$^+$-Mes]BF$_4$ (5 mol%) in 8 mL of acetone was irradiated with blue LED$_{456nm}$ light under O$_2$ at rt for 1 h. Yields were determined after purification.


Scheme 4 Gram-scale synthesis of imide 2a.

Table 2 Evaluation of green chemistry metrics for the synthesis of 2a

Reactant	1a	1.3 g	5 mmol	FW 273.38
Acid	AcOH	1.5 g	25 mmol	FW 60.05
Solvent	Acetone	25.51	—	—
Recycled solvent	Acetone	15.75	—	—
Product	2a	0.97 g	3.22 mmol	FW 301.35

These results clearly confirmed that the α-oxygenation reaction proceeded *via* the superoxide radical anion pathway.

To understand the photocatalytic reaction mechanism of the [Acr$^+$-Mes]BF$_4$ photocatalyst, absorption and emission spectra were recorded to perform a Stern–Volmer plot analysis. Initially, the excitation and emission of [Acr$^+$-Mes]BF$_4$ were recorded, using a photoluminescence spectrometer, to identify the maximum absorption and emission (Fig. 2). As shown in this figure, the excitation maximum and the emission maximum were at, respectively, 444 nm and 504 nm, which were used for further quenching experiments.

Initially, the emission of the photocatalyst was recorded under an N$_2$ atmosphere and the resulting intensity was taken as I_0. Then, the effect of concentration of substrate 1a was examined. A solution with saturated air and another with molecular oxygen were also investigated. As shown in Fig. 3, the emission decreases as the concentration concentration of substrate 1a and on the concentration of saturated air and oxygen showed only a negligible change in emissions.
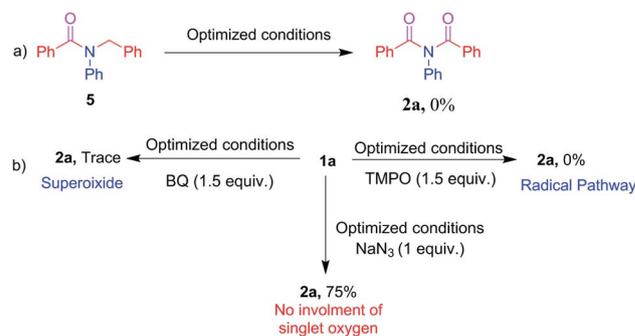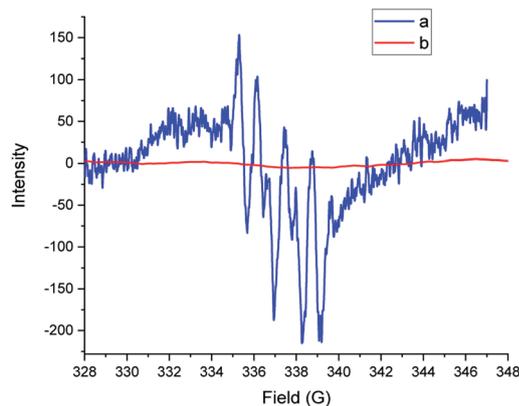

Scheme 5 Control and quenching experiments.

Fig. 1 Electron spin resonance (ESR) spectra of a solution of DMPO (20 μL) with **1a** (0.36 mmol), AcOH (1.8 mmol), and [Acr$^+$-Mes]BF$_4$ (5 mol%) in 8 mL acetone under O$_2$ at rt and (a) with blue LED$_{456nm}$ irradiation for 5 minutes and (b) without blue LED$_{456nm}$ irradiation.
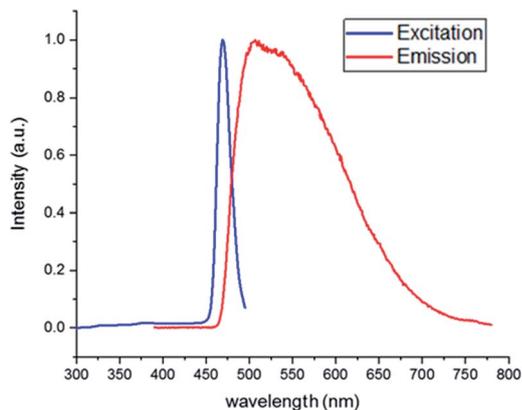

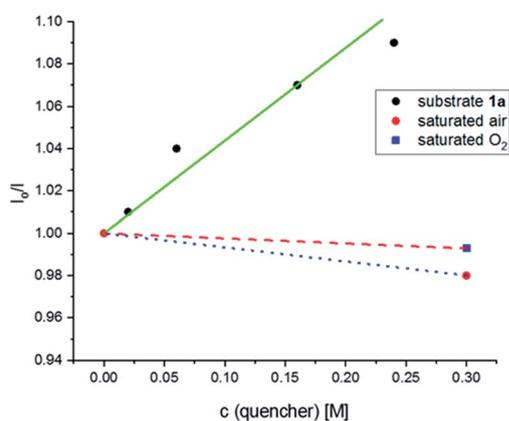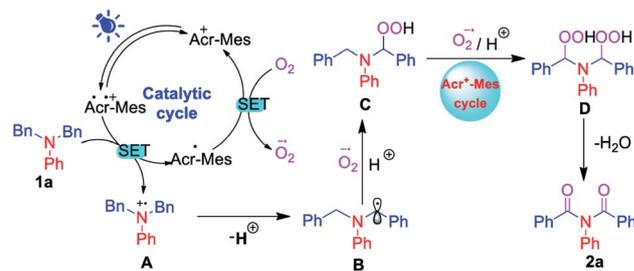**Fig. 2** Absorption–emission spectrum of [Acr$^+$-Mes]BF$_4$ in acetone.

Fig. 3 Stern–Volmer plot for oxygenation of N,N-dibenzylaniline **1a**.

Stern–Volmer quenching studies were performed to understand the catalytic cycle in the reaction mechanism (Fig. 3). The excited state of the Acr$^•$-Mes$^{•+}$ photocatalyst was quenched by applying N,N-dibenzylaniline **1a**. The

Scheme 6 A plausible mechanism of α-oxygenation for the synthesis of imides.

corresponding Stern–Volmer plot showed that there was a significant decrease in light emission intensity as the concentration of substrate **1a** was increased. In contrast, there was essentially no such change in the light emission intensity when either saturated air or molecular oxygen was added. These results clearly showed that the N,N-dibenzylaniline **1a** underwent reductive quenching with Acr$^•$-Mes$^{•+}$ in the catalytic cycle.

Based on the above experiments and literature reports,[24,26a] a possible reaction mechanism was sketched out, and is shown in Scheme 6. Initially, according to this mechanism, Acr$^+$-Mes was excited upon irradiation of visible light to form Acr$^•$-Mes$^{•+}$. Then, Acr$^•$-Mes$^{•+}$ underwent a single electron transfer process with **1a** to generate nitrogen radical cation A and Acr$^•$-Mes, and Acr$^•$-Mes was oxidized by O$_2$ via a single electron transfer process to generate a superoxide radical anion radical (O$_2^{•-}$) and it regenerated Acr$^+$-Mes. Then, the radical cation A lost H$^+$ to generate α-amino radical B. At that point, the hydroperoxide intermediate C was produced as a result of the nucleophilic attack on the amino radical B by in situ-generated O$_2^{•-}$ and H$^+$. Similarly, hydroperoxide intermediate C was converted to dihydroperoxide D in the catalytic cycle in the presence of blue LED light, followed by the nucleophilic addition of in situ-generated O$_2^{•-}$ and H$^+$. Finally, according to the proposed mechanism, imide **2a** was obtained from dihydroperoxide D as a result of the elimination of H$_2$O.

Conclusions

To summarize, we developed a visible-light-mediated direct α-oxygenation of N,N-dibenzylanilines to form imides in the presence of [Acr$^+$-Mes]BF$_4$ as a photocatalyst and molecular oxygen as a green oxidant. The α-oxygenation reaction method was operationally simple, and showed high atom economy and a low E-factor under mild conditions. Control and quenching experiments were also conducted and indicated the reaction mechanism to involve a radical pathway and superoxide radical anion, and also provided strong evidence for the reductive quenching of [Acr$^+$-Mes]BF$_4$ according to the acquired Stern–Volmer plot.

Conflicts of interest

There are no conflicts to declare.

Acknowledgements

Notes and references

1 S. M. Capitosti, T. P. Hansen and M. L. Brown, *Org. Lett.*, 2003, **5**, 2865–2867.

2 E. P. Balskus and E. N. Jacobsen, *J. Am. Chem. Soc.*, 2006, **128**, 6810–6812.

3 C. Takayama, O. Kirino, Y. Hisada and A. Fujinami, *Agric. Biol. Chem.*, 1987, **51**, 1547–1552.

4 Z. Cheng, X. Zhu, E. T. Kang and K. G. Neoh, *Macromolecules*, 2006, **39**, 1660–1663.

5 A. M. Higgins and R. A. L. Jones, *Nature*, 2000, **404**, 476–478.

6 J. Sperry, *Synth*, 2011, **2011**, 3569–3580.

7 M. B. Andrus, W. Li and R. F. Keyes, *Tetrahedron Lett.*, 1998, **39**, 5465–5468.

8 L. Xu, S. Zhang and M. L. Trudell, *Chem. Commun.*, 2004, 1668–1669.

9 C. S. Digwal, U. Yadav, P. V. S. Ramya, S. Sana, B. Swain and A. Kamal, *J. Org. Chem.*, 2017, **82**, 7332–7345.

10 J. S. P. Schwarz, *J. Org. Chem.*, 1972, **37**, 2906–2908.

11 K. Brady and A. F. Hegarty, *J. Chem. Soc., Perkin Trans. 2*, 1980, 121–126.

12 O. Mumm, H. Hesse and H. Volquartz, *Ber. Dtsch. Chem. Ges.*, 1915, **48**, 379–391.

13 K. C. Nicolaou and C. J. N. Mathison, *Angew. Chem.*, 2005, **117**, 6146–6151.

14 K. Kataoka, K. Wachi, X. Jin, K. Suzuki, Y. Sasano, Y. Iwabuchi, J.-y. Hasegawa, N. Mizuno and K. Yamaguchi, *Chem. Sci.*, 2018, **9**, 4756–4768.

15 A. Schnyder and A. F. Indolese, *J. Org. Chem.*, 2002, **67**, 594–597.

16 H. Q. Li, K. W. Dong, H. Neumann and M. Beller, *Angew. Chem., Int. Ed.*, 2015, **54**, 10239–10243.

17 Y. Li, K. Dong, F. Zhu, Z. Wang and X.-F. Wu, *Angew. Chem., Int. Ed.*, 2016, **55**, 7227–7230.

18 P. Nagaraaj and V. Vijayakumar, *Org. Chem. Front.*, 2019, **6**, 2570–2599.

19 H. Yu and Y. Zhang, *Eur. J. Org. Chem.*, 2015, **2015**, 1824–1828.

20 H. Yu, Y. Chen and Y. Zhang, *Chin. J. Chem.*, 2015, **33**, 531–534.

21 S. Biswas, H. S. Khanna, Q. A. Nizami, D. R. Caldwell, K. T. Cavanaugh, A. R. Howell, S. Raman, S. L. Suib and P. Nandi, *Sci. Rep.*, 2018, **8**, 13649–13656.

22 V. P. Charpe, A. Ragupathi, A. Sagadevan and K. C. Hwang, *Green Chem.*, 2021, **23**, 5024–5030.

23 (*a*) Y. Zhang, W. Schilling, D. Riemer and S. Das, *Nat. Protoc.*, 2020, **15**, 822–839; (*b*) S. Zhu, A. Das, L. Bui, H. Zhou, D. P. Curran and M. Rueping, *J. Am. Chem. Soc.*, 2013, **135**, 1823–1829.

24 Y. Zhang, D. Riemer, W. Schilling, J. Kollmann and S. Das, *ACS Catal.*, 2018, **8**, 6659–6664.

25 I. Itoh, Y. Matsusaki, A. Fujiya, N. Tada, T. Miura and A. Itoh, *Tetrahedron Lett.*, 2014, **55**, 3160–3162.

26 (*a*) M. Bhargava Reddy, N. Neerathilingam and R. Anandhan, *Org. Chem. Front.*, 2021, **8**, 87–93; (*b*) M. Bhargava Reddy, K. Prasanth and R. Anandhan, *Org. Biomol. Chem.*, 2020, **18**, 9601–9605; (*c*) M. Bhargava Reddy and R. Anandhan, *Chem. Commun.*, 2020, **56**, 3781–3784; (*d*) N. Neerathilingam, M. Bhargava Reddy and R. Anandhan, *J. Org. Chem.*, 2021, **86**, 15117–15127; (*e*) K. Prasanth, M. Bhargava Reddy and R. Anandhan, *Asian J. Org. Chem.*, 2022, **11**, e202100590.

27 A. Sagadevan, P.-C. Lyu and K. C. Hwang, *Green Chem.*, 2016, **18**, 4526–4530.

28 (*a*) Y. Zhang, W. Schilling and S. Das, *ChemSusChem*, 2019, **12**, 2898–2910; (*b*) W. Schilling, Y. Zhang, D. Riemer and S. Das, *Chem.–Eur. J.*, 2020, **26**, 390–395; (*c*) J. Kollmann, Y. Zhang, W. Schilling, T. Zhang, D. Riemer and S. Das, *Green Chem.*, 2019, **21**, 1916–1920; (*d*) Y. Zhang, N. Hatami, N. S. Lange, E. Ronge, W. Schilling, C. Jooss and S. Das, *Green Chem.*, 2020, **22**, 4516–4522.

29 X. Ling, Y. Xiong, R. Huang, X. Zhang, S. Zhang and C. Chen, *J. Org. Chem.*, 2013, **78**, 5218–5226.